



Creation of Ultra-Long Pure Magnetization Needle By circularly Polarized Beam with A Ternary Optical Element

M. Udhayakumar¹, Haresh M Pandya², K. B. Rajesh^{3*}

^{1,2,*3} Department of Physics, Government Arts College, Tiruppur, Tamilnadu, India

Received: 21.08.2019 Accepted: 25.09.2018

Abstract

Based on the vector diffraction theory and Inverse Faraday Effect, the light induced magnetization needle is generated by tightly focusing a circularly polarized beam that is modulated by a self-designed ternary hybrid (phase/amplitude) filter (THF). Both the phase and the amplitude patterns of THF are judiciously optimized by the versatile particle swarm optimization (PSO) searching algorithm. It is noted that by optimizing to produce an ultra-long pure magnetization needle with lateral sub-wavelength scale and a super-long spherical magnetization chain with three-dimensional super resolution. The present work regarding these super-resolution magnetization patterns is of great value in high density all-optical magnetic recording, atomic trapping as well as confocal and magnetic resonance microscopy.

Keywords: Azimuthally polarized beam; Diffractive Optical Element; Super-Resolution.

1. INTRODUCTION

The ultra-fast response of the light induced magnetization field in the magneto optical film is great interest in the recent year owing to its potential application in all-optical magnetic recording (AOMR) (Stanciu *et al.* 2007; Khorsand *et al.* 2012; Mangin *et al.* 2014), confocal and magnetic resonance microscopy (Grinolds *et al.* 2014), atom trapping (Vetsch *et al.* 2010; Schneeweiss *et al.* 2014), and multi-dimensional magneto-optical data storage (Zijlstra *et al.* 2009; Gu *et al.* 2014). All these application demands a pure longitudinal magnetization focal structure which allows a well-defined magnetization direction in a material on an ultra-small 3D volume beyond the diffraction limit ($\sim \lambda^3/8$). Such a magnetization focal structure is vital for applications including high-density magnetic-optical data storage and high-resolution magnetic resonance microscopy. Apart from this, spherical 3D super resolution spot multiple into an array is a strategy demand to enhance the processing speed and power efficiency of the magneto optical recording and also essential for multiple magnetic particle trapping and manipulation. In this respect, numerous endeavors have been devoted to tailor the magnetization structure through manipulating the mutual interaction between

the polarization singularities of cylindrical polarization beam and optical vortex (Jiang *et al.* 2013; Qin *et al.* 2015; Gong *et al.* 2016; Yan *et al.* 2017; Sicong Wang *et al.* 2018), in conjunction with amplitude/phase modulation (Wang *et al.* 2014; Nie *et al.* 2015; Ma *et al.* 2015; Yan *et al.* 2017a, 2017b; Udhayakumar *et al.* 2018a; 2018b). The tightly focused circularly polarized beam with a high numerical aperture objective has been considered as an effective method to generate and reverse the longitudinal magnetization in the magnetic material up on changing the handedness of a circularly polarized beam (Savoini *et al.* 2012; El Hadri *et al.* 2016a, 2016b, 2017; Pierre Vallobra *et al.* 2017; Quessab *et al.* 2018). Recently, Particle swarm optimization (PSO) algorithm, which is inspired by the emergent motion of a flock of birds hunting for food, has become a powerful tool to determine the parameters of DOEs for improving the performances of optical fields (Jie Lin *et al.* 2016; Mohamed Ahmed Mohandes, 2012). It is manifested that the PSO performs well in finding good solution to optimize the objective function. In contrast to other optimization techniques, the PSO has better search performance with faster and more stable convergence rates (Ioan Cristian Trelea, 2003). Although this novel optimization scheme has several merits, such as global optimization, fast

* K. B. Rajesh

email: rajeshkb@gmail.com

convergence and reduced iteration number, the combination of both the generic algorithm and PSO one will make the whole optimization system more complex (Jie Lin *et al.* 2016; Mohamed Ahmed Mohandes, 2012). Here we numerically demonstrate, based on VDT and IFE, the possibility of inducing highly confined magnetization field the extends up to 10.2λ with no side lobes and exceptionally much reduced transverse magnetization component. We also illustrated the magnetization spots that extends axially using a circularly polarized annular multi Gaussian beam by a self-designed ternary hybrid (phase/amplitude) filter (THF) and focused by high NA objective.

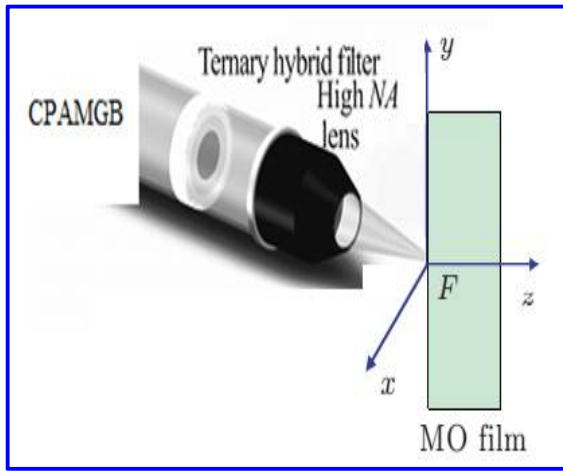


Fig. 1: Schematic setup to generate the pure longitudinal magnetization needle using circularly polarized annular multi Gaussian beam (CPAMGB) with THF.

2. THEORY

The schematic of the proposed method is shown in Fig (1). In a tight focusing system, amplitude of the multi-Gaussian beam at the entrance plane ($z_0=0$), in cylindrical coordinate system (ρ, ϕ, z_0), can be written as (Jian-Nong *et al.* 2011)

$$P(\theta) = \left(\frac{\theta}{\theta_0} \right)^m \sum_{n=-N}^N \exp \left[- \left(\frac{\theta - \theta_c - n\omega_0}{\omega_0} \right)^2 \right] \quad (1)$$

Here, θ is the converging semi-angle. θ_{\max} maximum converging semi-angle as which is related to objective numerical aperture by $\theta_{\max} = \arcsin(NA)$. θ_0 is an angle which, along with integer m , determines the shape of the modulation function. θ_0 is usually chosen to be slightly smaller than θ_{\max} . θ_c determines the radial position translation of $P(\theta)$. Here we take $\theta_c = \theta_{\max}/2$. w_0 is the waist width of single Gaussian beam which is calculated by the following formula

$$w_0 = 1/2 \times \frac{\theta_{\max}}{N + \left\{ 1 - \ln \left[\sum_{n=-N}^N \exp(-n^2) \right] \right\}^{1/2}} \quad (2)$$

Equation (1) describes an object beam. It is suitable to convert Eq. (1) from a function of angle into a function of radial polar coordinate. One may substitute θ with $\arcsin(r/f)$, where f is the focal distance of the objective. In Eq. (1), the factor (θ/θ_0) measures that the most of light energy is located on the annular edge of the pupil. Increasing the integer m concentrates more energy into the annular edge area in which the converging semi-angle is more than θ_0 . The sum of $(2N + 1)$ spatially equally spaced Gaussian beams ensures that amplitude of the constructed annular multi-Gaussian beam decreases suddenly, when reaching the outer edge of the pupil. Such an amplitude modulated beam can be realized by encoding suitable phase mask on spatial light modulator. Based on Richards and Wolf's vectorial diffraction method widely used for high NA focusing systems at arbitrary incident polarization (Richards and Wolf, 1959) the electric field $E(\rho, \phi, z)$ in the vicinity of the focal region of an incident circularly polarized beam can be written as.

$$E_{cir}^L(\rho_c, \phi_c, z_c) = \begin{bmatrix} i e_x + e'_x \\ i e_y + e'_y \\ i e_z + e'_z \end{bmatrix} = \begin{bmatrix} A(T_0 + T_2 e^{-i2\phi_c}) \\ -iA(T_0 - T_2 e^{-i2\phi_c}) \\ -2iA T_1 e^{-i2\phi_c} \end{bmatrix} \quad (3)$$

Where

$$\begin{aligned}
 T_0 &= \int_0^\alpha (1 + \cos \theta) \sqrt{\cos \theta} P(\theta) A(\theta) \sin \theta J_0(k \rho_c \sin \theta) \exp(ik z_c \cos \theta) d\theta \\
 T_1 &= \int_0^\alpha \sin^2 \theta \sqrt{\cos \theta} P(\theta) A(\theta) J_1(k \rho_c \sin \theta) \exp(ik z_c \cos \theta) d\theta \\
 T_2 &= \int_0^\alpha (1 - \cos \theta) \sqrt{\cos \theta} P(\theta) A(\theta) \sin \theta J_2(k \rho_c \sin \theta) \exp(ik z_c \cos \theta) d\theta
 \end{aligned} \tag{4}$$

Here α is the convergence semi angle of the lens, $k=2\pi/\lambda$ is the wave number, A is a constant, and J_n is the n th Bessel function of the first kind. The magnetization can be induced by the inverse Faraday Effect. For simplicity, the conducting electrons in the magneto optical film can be treated as a collision less plasma in which the electrons can move freely, at least on the time scale given by the period of the high-frequency field and the wave's fluctuating magnetic field is neglected. Thus the magnetization M generated in the plasma by the high-frequency field is proportional to $iE \times E^*$ (Van der Ziel *et al.* 1965), which can be expressed as (Hertel, 2006; Volkov and Novikov, 2002)

$$M(\rho_c, \phi_c, z_c) = i\gamma E \times E^* \tag{5}$$

Where γ is a magneto optical constant. Substituting Eq. (3-4) into Eq.(5) we obtain the magnetization M_n normalized to γA and for the incident left-handed circularly polarized light that is given by

$$M_n^L(\rho_c, \phi_c, 0) = \frac{M_n^L(\rho_c, \phi_c, 0)}{\gamma A} \begin{bmatrix} -4T_1(T_0 + T_2 \sin \phi_c) \\ 4T_1(T_0 + T_2 \cos \phi_c) \\ -2(T_0^2 - T_2^2) \end{bmatrix} \tag{6}$$

From Eqs. (6), one can immediately see that the magnetization is a three-dimensional distribution in general.

3. NUMERICAL SIMULATION RESULTS AND DISCUSSION

The fixed parameters used for the calculations are $\lambda = 1$, and $NA = 0.85$. Here, for simplicity, we assume that the refractive index $n = 1$ and order (m) of CPAMGB as 30. For all calculation in the length unit is normalized to λ and the energy density is normalized to unity. Fig 2(a) shows the 2D magnetization distribution obtained for the incident CPAMGB with $m=30$. Fig 2(b) and (c) shows the corresponding magnetization distribution in the radial and axial planes. We noted for the fig 2(b) and (c) the FWHM of the magnetization spots is 0.45λ and its focal depth is 8λ . we also noted that the residual radial magnetization distribution is only 10% of the longitudinal distribution and there are no side lobes observed. Hence such a magnetization spot can be utilized for all optical helical switching.

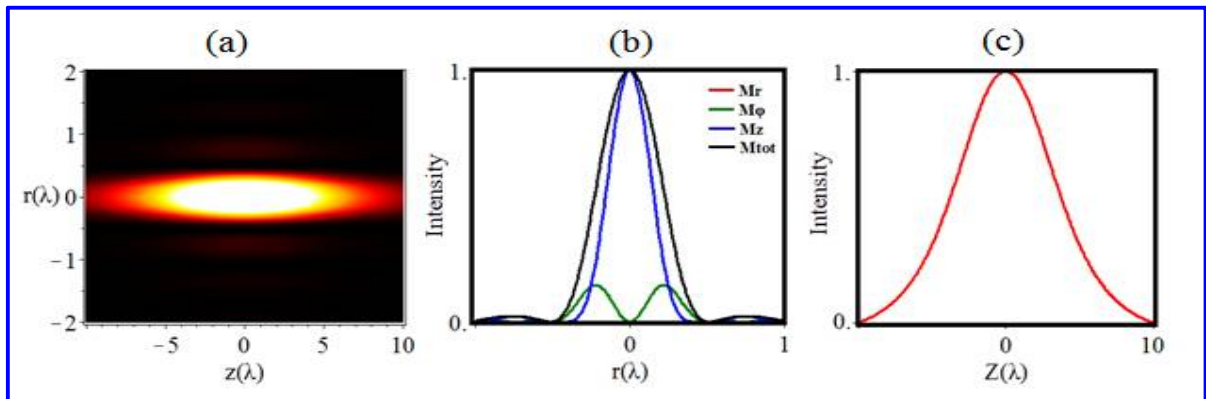


Fig. 2: (a) 2D Normalized magnetization distribution in r - z plane for circularly polarized annular multi-Gaussian beams ($m = 30$). (b) Normalized magnetization profiles along the radial direction at $z = 0$. (c) Magnetization profiles along the z -axis at $r = 0$.

However it is very much essential to improve the focal depth of the magnetization spot without increasing the spot size. However for helical depended switching, the incident beam should be of circularly polarized and here we demonstrated the possibility of creating the super long magnetization needle of sub wavelength scale magnetization spots using a novel sine-shaped ternary hybrid filter (THF) is well devised with the modified PSO algorithm to produce a pure longitudinally magnetization needle with ultra-long DOF by strongly focused a circularly polarized annular multi Gaussian beam (CPAMGB).

$$A(\theta) = \sum_{i=0}^m p_i \sin(2\pi s_i / \alpha)$$

Is the transmittance function with p_i , s_i and m being the radius and phase factors and the belts number of the-THFs (Xiaoyu Weng *et al.* 2014). It should be mentioned that, different from the common binary DOE, we can controllably vary both the amplitude (0—1) and the phase ($0/\pi$) of THF. Moreover, the proposed PSO algorithm is able to robustly solve the multiple parameters of the THF with fast convergence and global optimum.

Table 1. Parameters of the sine-shaped ternary hybrid filter for $m=2$

Order of belts	First	Second	Third
Normalized transmittance	1.024	2.041	3.070
Phase parameter	1	0.183	0.278
Amplitude parameter	0.725	1.216	1.158

Fig 3(a) shows that generating subwavelength scale magnetization probe with fine axial homogeneity generated by Fig 3(b) shows that the FWHM of the generated magnetic probe is 0.4λ . The on axial intensity distribution shows in fig 4(c) shows that the generated magnetization focal segment is axially homogenous and its FWHM the DOF is around 6.4λ . Thus by using a single focusing unit and by properly axial field strength is achieved in the focal region. The perfect magnetization needle and the accessible method give a guide for ultrahigh density magnetic storage, fabricating magnetic lattices for spin wave operation as well as atomic trapping.

Fig. 4(a), shows the 2D magnetization distribution obtained for the incident CPAMGB with $m=30$. It is noted from fig 4(b) the FWHM of generated magnetization spot is only 0.4λ with no side lobe and the residual transverse magnetization is still 5% of the longitudinal magnetization distribution. It is noted from fig. 4(c), the depth of focus (DOF) of the generated magnetization spot very well extended up to 10.2λ . Moreover, since the HGPSO combines the genetic algorithm, self-adaptive parameters, recombination and mutation operation (Jie Lin *et al.* 2016), the program structure of the HGPSO is more complex than that of PSO, thus leading to low optimization search efficiency in multi-dimensional data optimization. In these regards, our proposed PSO is a feasible and efficient way to design and optimize the filters for achieving the magnetization needle. Such a subwavelength scale needle of longitudinal magnetization spot find applications for ultrahigh density magnetic storage, fabricating magnetic lattices for spin wave operation, as well as atomic trapping.

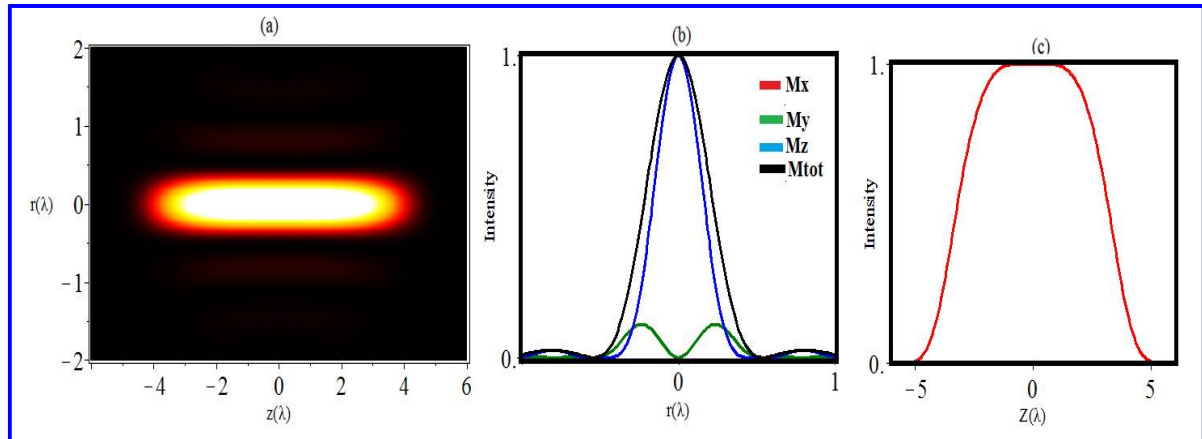


Fig. 3: (a) 2D Normalized Super-long magnetization needle with well axial homogeneity ($m = 2$). (b) Normalized magnetization profiles along the radial direction at $z = 0$. (c) Magnetization profiles along the z -axis at $r = 0$.

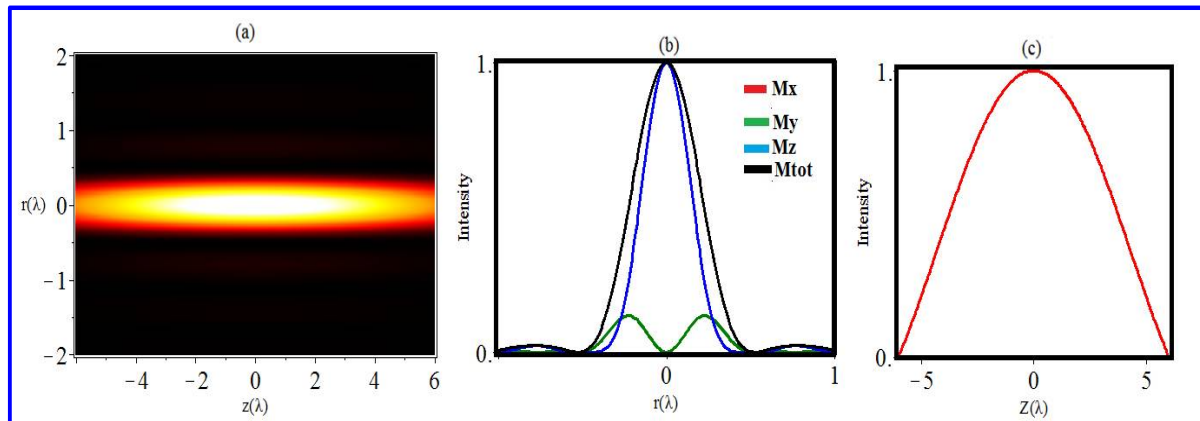


Fig. 4. (a) 2D Normalized magnetization needle for circularly polarized annular multi-Gaussian beams with THF. When ($m = 30$). (b) Normalized magnetization profiles along the radial direction at $z = 0$. (c) Magnetization profiles along the z -axis at $r = 0$.

4. CONCLUSIONS

Based on the vector diffraction theory and Inverse Faraday Effect, the light induced magnetization needle is generated by tightly focusing a circularly polarized annular multi Gaussian beam that is modulated by a self-designed ternary hybrid (phase/amplitude) filter (THF). Both the phase and the amplitude patterns of THF are judiciously optimized by the versatile particle swarm optimization (PSO) searching algorithm. It is noted that by optimized sine-shaped THFs to produce an ultra-long pure magnetization needle with lateral sub-wavelength scale, an magnetization needle with the full width at half maximum (FWHM) of 0.4λ and the DOF of 10.2λ is achieved. The pure longitudinal magnetization needle with super high aspect ratio and well axial uniformity for ultrahigh density all-optical magnetic recording and fabricating magnetic lattices for spin wave operation and atomic trapping with flexibility.

REFERENCES

- El Hadri, M. S., Michel Hehn, Philipp Pirro, Charles-Henri Lambert, Grégory Malinowski, Eric E. Fullerton and Stéphane Mangin, Domain size criterion for the observation of all-optical helicity-dependent switching in magnetic thin films, *Phys. Rev. B.*, 94(6), 064419(2016b).
[doi:10.1103/PhysRevB.94.064419](https://doi.org/10.1103/PhysRevB.94.064419)
- El Hadri, M. S., Pirro, P., Lambert, C.-H., Bergeard, N., Petit-Watlot, S., Hehn, M., Malinowski, G., Montaigne, F., Quessab, Y., Medapalli, R., Fullerton, E. E. and Mangin, S., Electrical characterization of all-optical helicity-dependent switching in ferromagnetic Hall crosses, *Appl. Phys. Lett.*, 108, 092405-5(2016a).
[doi:10.1063/1.4943107](https://doi.org/10.1063/1.4943107)
- Gong, L., Wang, L., Zhu, Z., Wang, X., Zhao, H. and Gu, B., Generation and manipulation of super-resolution spherical magnetization chains, *Appl. Opt.*, 55(21), 5783–5789(2016).
[doi:10.1364/AO.55.005783](https://doi.org/10.1364/AO.55.005783)
- Grinolds, M. S., Warner, M., De Greve, K., Dovzhenko, Y., Thiel, L., Walsworth, R. L., Hong, S., Maletinsky, P. and Yacoby, A., Subnanometre resolution in three-dimensional magnetic resonance imaging of individual dark spins, *Nat Nanotechnol.*, 9(4), 279-284(2014).
[doi: 10.1038/nnano.2014.30](https://doi.org/10.1038/nnano.2014.30)
- Gu, M., Xiangping Li and Yaoyu Cao, Optical storage arrays: a perspective for future big data storage, *Light: Sci. Appl.*, 3, e177(2014).
[doi:10.1038/lsa.2014.58](https://doi.org/10.1038/lsa.2014.58)
- Hadri, M. S., Hehn Michel, Malinowski Gregory, Mangin Stéphane, Materials and devices for all-optical helicity-dependent switching, *J. Phys. D: Appl. Phys.*, 50(13), 133002(2017).
[doi:10.1088/1361-6463/aa5adf](https://doi.org/10.1088/1361-6463/aa5adf)
- Hertel, R., Theory of the inverse Faraday Effect in metals, *J. Magn. Magn. Mater.*, 303(1), L1–L4(2006).
[doi:10.1016/j.jmmm.2005.10.225](https://doi.org/10.1016/j.jmmm.2005.10.225)
- Ioan Cristian Trelea, The particle swarm optimization algorithm: convergence analysis and parameter selection, *Information Processing Letters*, 85(6), 317-325(2003).
[doi:10.1016/S0020-0190\(02\)00447-7](https://doi.org/10.1016/S0020-0190(02)00447-7)
- Jiang, Y., Li, X. and Gu, M., Generation of sub-diffraction-limited pure longitudinal magnetization by the inverse Faraday effect by tightly focusing an azimuthally polarized vortex beam, *Opt. Lett.*, 38(16), 2957–2960(2013).
[doi:10.1364/OL.38.002957](https://doi.org/10.1364/OL.38.002957)

- Jian-Nong, C., Qin-Feng, X. and Gang, W., Tight focus of a radially polarized and amplitude-modulated annular multi-Gaussian beam, *Chin. Phys. B20*, 114211 (2011).
[doi:10.1088/1674-1056/20/11/114211](https://doi.org/10.1088/1674-1056/20/11/114211)
- Jie Lin, Hong-yang Zhao, Yuan Ma, Jiubin Tan and Peng Jin, New hybrid genetic particle swarm optimization algorithm to design multi-zone binary filter, *Optics Express*, 24(10), 10748-10758(2016).
[doi:10.1364/OE.24.010748](https://doi.org/10.1364/OE.24.010748)
- Khorsand, A. R., Savoini, M., Kirilyuk, A., Kimel, A. V., Tsukamoto, A., Itoh, A. and Rasing, Th., Role of magnetic circular dichroism in all-optical magnetic recording, *Phys. Rev. Lett.*, 108(12), 127205(2012).
[doi:10.1103/PhysRevLett.108.127205](https://doi.org/10.1103/PhysRevLett.108.127205)
- Ma, W., Zhang, D., Zhu, L. and Chen, J., Super-long longitudinal magnetization needle generated by focusing an azimuthally polarized and phase-modulated beam, *Chin. Opt. Lett.*, 13(5), 52101–52105(2015).
- Mangin, S., Gottwald, M., Lambert, C., Steil, D., Uhlř, V., Pang, L., Hehn, M., Alebrand, S., Cinchetti, M., Malinowski, G., Fainman, Y., Aeschlimann, M. and Fullerton, E. E., Engineered materials for all-optical helicity-dependent magnetic switching, *Nat. Mater.* 13, 286–292(2014).
[doi:10.1038/nmat3864](https://doi.org/10.1038/nmat3864)
- Mohamed Ahmed Mohandes, Modeling global solar radiation using particle swarm optimization (PSO), *Solar Energy* 86(11), 3137-3145(2012).
[doi:10.1016/j.solener.2012.08.005](https://doi.org/10.1016/j.solener.2012.08.005)
- Nie, Z., Ding, W., Shi, G., Li, D., Zhang, X., Wang, Y. and Song, Y., Achievement and steering of light-induced sub-wavelength longitudinal magnetization chain, *Opt. Express*, 23(16), 21296–21305(2015).
[doi:10.1364/OE.23.021296](https://doi.org/10.1364/OE.23.021296)
- Pierre Vallobra, Thibaud Fache, Yong Xu, Lei Zhang, Gregory Malinowski, Michel Hehn, Juan-Carlos Rojas-Sánchez Eric.E. Fullerton and Stephane Mangin, Manipulating exchange bias using all-optical helicity-dependent switching, *Phys. Rev. B.*, 96, 144403(2017).
- Qin, F., Huang, K., Wu, J., Jiao, J., Luo, X., Qiu, C. and Hong, M., Shaping a subwavelength needle with ultra-long focal length by focusing azimuthally polarized light, *Sci. Rep.*, 5, 9977(2015).
[doi: 10.1038/srep09977](https://doi.org/10.1038/srep09977)
- Quessab, Y., Medapalli, R., El Hadri, M. S., Hehn, M., Malinowski, G., Fullerton, E. E. and Mangin, S., Helicity-dependent all-optical domain wall motion in ferromagnetic thin films, *Phys. Rev. B.*, 97(5), 054419(2018).
[doi:10.1103/PhysRevB.97.054419](https://doi.org/10.1103/PhysRevB.97.054419)
- Richards, B. and Wolf, E., Electromagnetic diffraction in optical systems, II. Structure of the image field in an aplanatic system, *Proc. Roy. Soc. A* 253, 358–379 (1959).
[doi:10.1098/rspa.1959.0200](https://doi.org/10.1098/rspa.1959.0200)
- Savoini, M., Medapalli, R., Koene, B., Khorsand, A. A., Le Guyader, L., Duo, L., Finazzi, M., Tsukamoto, A., Itoh, A., Nolting, F., Kirilyuk, A., Kimel, A. V. and Rasing, Th., Highly efficient all-optical switching of magnetization in GdFeCo microstructures by interference-enhanced absorption of light, *Phys. Rev. B.*, 86, 140404(R)(2012).
[doi:10.1103/PhysRevB.86.140404](https://doi.org/10.1103/PhysRevB.86.140404)
- Schneeweiss, P., Le Kien, F. and Rauschenbeutel, A., Nanofiber-based atom trap created by Combining fictitious and real magnetic fields, *New J. Phys.*, 16, 013014(2014).
[doi:10.1088/1367-2630/16/1/013014](https://doi.org/10.1088/1367-2630/16/1/013014)
- Sicong Wang, Chen Wei, Yuanhua Feng, Yaoyu Cao, Haiwei Wang, Weiming Cheng, Changsheng Xie, Arata Tsukamoto, Andrei Kirilyuk, Theo Rasing, Alexey V. Kimel and Xiangping Li, All-optical helicity-dependent magnetic switching by first-order azimuthally polarized vortex beams, *Appl. Phys. Lett.*, 113, 171108(2018).
[doi:10.1063/1.5051576](https://doi.org/10.1063/1.5051576)
- Stanciu, C. D., Hansteen, F., Kimel, A. V. and Kirilyuk Tsukamoto, A., All-optical magnetic recording with circularly polarized light, *Phys. Rev. Lett.*, 99(4), 047601-047606(2007).
[doi:10.1103/PhysRevLett.99.047601](https://doi.org/10.1103/PhysRevLett.99.047601)
- Udhayakumar, M., Prabakaran, K. and Rajesh, K. B., Generation of Ultra-Long Pure Magnetization Needle and Multiple Spots by Phase Modulated Doughnut Gaussian Beam, *Optics and Laser Technology*, 102, 40-46,(2018b).
[doi:10.1016/j.optlastec.2017.12.008](https://doi.org/10.1016/j.optlastec.2017.12.008)
- Udhayakumar, M., Prabakaran, K., Rajesh, K. B., Jaroszewicz, Z. and Belafhal, A., Generating Sub wavelength pure longitudinal magnetization probe and chain using complex phase plate. *Optic Communication*, 407, 275–279,(2018a).
[doi:10.1016/j.optcom.2017.09.007](https://doi.org/10.1016/j.optcom.2017.09.007)
- Van der Ziel, J. P., Peter S. Pershan and Malmstrom, L. D., Optically-induced magnetization resulting from the inverse Faraday Effect, *Phys. Rev. Lett.*, 15(5), 190–193(1965).
[doi:10.1103/PhysRevLett.15.190](https://doi.org/10.1103/PhysRevLett.15.190)
- Vetsch, V., Reitz, D., Sague, G., Schmidt, R., Dawkin, S. T. and Rauschenbeutel, A., Optical interface created by Laser-cooled atoms trapped in the evanescent field surrounding an optical nanofiber, *Phys. Rev. Lett.*, 104(20), 203603(2010).
[doi:10.1103/PhysRevLett.104.203603](https://doi.org/10.1103/PhysRevLett.104.203603)

- Volkov, P. V. and Novikov, M. A., Inverse Faraday Effect in anisotropic media, *Crystallography Rep.*, 47(5), 824–828, (2002).
[doi:10.1134/1.1509399](https://doi.org/10.1134/1.1509399)
- Wang, S., Li, X., Zhou, J. and Gu, M., Ultra long pure longitudinal magnetization needle induced by annular vortex binary optics, *Opt. Lett.*, 39(17), 5022–5025 (2014).
[doi:10.1364/OL.39.005022](https://doi.org/10.1364/OL.39.005022)
- Xiaoyu Weng, Xiumin Gao, Hanming Guo and Songlin Zhuang, Creation of tunable multiple 3D dark spots with cylindrical vector beam, *Applied Optics.*, 53(11), 2470-2476(2014).
[doi:10.1364/AO.53.002470](https://doi.org/10.1364/AO.53.002470)
- Yan, W., Nie, Z., Zhang, X., Wang, Y. and Song, Y., Magnetization shaping generated by tight focusing of azimuthally polarized vortex multi-Gaussian beam, *Appl. Opt.*, 56(7), 1940–1946(2017).
[doi:10.1364/AO.56.001940](https://doi.org/10.1364/AO.56.001940)
- Yan, W., Nie, Z., Zhang, X., Wang, Y. and Song, Y., Generation of an ultra-long pure longitudinal magnetization needle with high axial homogeneity using an azimuthally polarized beam modulated by pure multi-zone plate phase filter, *J. Opt.*, 19(8), 085401(2017a).
[doi:10.1088/2040-8986/aa73ce](https://doi.org/10.1088/2040-8986/aa73ce)
- Yan, W., Nie, Z., Zhang, X., Wang, Y. and Song, Y., Theoretical guideline for generation of an ultra-long magnetization needle and a super-long conveyed spherical magnetization chain, *Optics Express*, 25(19), 22268-22279(2017b).
[doi:10.1364/OE.25.022268](https://doi.org/10.1364/OE.25.022268)
- Zijlstra, P., Chon, J. W. and Gu, M., Five-dimensional optical recording mediated by surface Plasmon's in gold Nano rods, *Nature*, 459(7245), 410-413(2009).
[doi:10.1038/nature08053](https://doi.org/10.1038/nature08053)